RSC Advances

RSC Publishing

PAPER

Accurate polarity control and parallel alignment of actin filaments for myosin-powered transport systems†

Cite this: *RSC Advances*, 2013, **3**, 8728

Makito Miyazaki,[a] Kazuhiko Kinosita Jr[a] and Katsuyuki Shiroguchi*[b]

Received 14th August 2012,
Accepted 20th March 2013

DOI: 10.1039/c3ra41112e

www.rsc.org/advances

An actin filament is a micrometer-long biological filament, which serves as a track of transport systems in cells. The filament exhibits polarity while myosin transports a cargo along it unidirectionally. Here, we established a method to align many actin filaments parallel with each other on a substrate with uniform (>99%) polarity as assessed by myosin movements. This actin array is an ideal candidate for the construction of a nano-scale unidirectional transport system powered by myosin.

Introduction

The micro total analysis system (μTAS) is a device that miniaturizes several experimental systems for chemical or biochemical analysis on the micrometer scale and integrates them on a single chip.[1–4] For instance, real-time PCR (polymerase chain reaction),[5] cell sorting,[6] immunoassay,[7] and drug discovery[8] assays are performed on such a chip. Such a device enables high-throughput analysis and thus it is utilized in a wide range of fields from molecular biology to medical research.

The main component of the device is a micrometer-scale flow channel. Target molecules are transported inside the channel. By accurate control of the fluid pressure using a syringe pump, sub-picoliter volumes of sample may be quickly and precisely transported in the channel. To increase the device throughput, further downsizing of the flow channel has been desired. However, the conventional transport method utilizing a syringe pump is inappropriate for smaller (nanometer) scales because the large fluid resistance makes the flow speed abruptly slow on the nano-scale.[9,10]

To transport target molecules in a nano-scale channel efficiently, reconstituting a biological transport system in a fluidic device has been regarded as a possible approach because nano-scale transport is well performed within cells.[11–14] The biological transport system essentially consists of vesicles, motor proteins, and protein filaments. Target molecules are encapsulated in submicron-sized vesicles and nanometer-sized motor proteins transport the vesicles along micrometer-long protein filaments, which is driven by ATP, an energy source in the cell. The protein filament exhibits structural polarity, and the motor protein recognizes the polarity and moves unidirectionally along the filament. In cells, the alignment and polarity of the filaments control the direction of transport. To apply this biological function for the nano-scale transport system, in which many target molecules are transported undirectionally along multiple filaments, the following technique is essential: polarity control of protein filaments and parallel immobilization of the multiple filaments on a substrate without the loss of their biological function as a track used by the motor protein.

Both, actin filaments and microtubules are known to be suitable tracks for motors protein movement.[14,15] An actin filament is a semi-flexible polymer of 6 nm in diameter.[15] The filament is formed by self-assembly of actin monomers and exhibits twisted two-stranded configuration. Flexibility of the filament is explained by the persistent length: l_p = 15–20 μm.[16–19] In contrast, a microtubule is a rigid tube-like rod of 25 nm in diameter, co-assembled by α and β tubulin subunits[15] and with l_p = 5000–6000 μm.[20] Both filaments have ''plus'' and ''minus'' ends, which determine the structural polarity. Recently, isopolar arrays of microtubules have been successfully constructed, and unidirectional transport systems powered by microtubule-associated motor protein kinesin have been proposed.[9,10,21–24] Therefore, development of actin-myosin transport systems is essential to integrate two independent biological transport systems (actin- and microtubule-based systems) on a single chip, which allows nano-scale sorting of target molecules by the specific interaction between motor proteins and their tracks.

In this article, we propose an efficient method to fabricate isopolar parallel arrays of actin filaments that act as a track for myosin. The idea of this method is based on the following three reports. Huang *et al.*[25] controlled the polarity of actin filaments by anchoring the filaments on the substrate through gelsolin, an actin capping protein that severs the actin filament and caps the generated plus end of the filament.[26]

[a]*Department of Physics, Faculty of Science and Engineering, Waseda University, Tokyo, 169-8555, Japan*
[b]*Laboratory for Integrative Genomics, RCAI, RIKEN Center for Integrative Medical Sciences (IMS-RCAI), Yokohama, 230-0045, Japan.*
E-mail: katsuyuki.shiroguchi@riken.jp

† Electronic supplementary information (ESI) available: One supplementary text and one movie. See DOI: 10.1039/c3ra41112e

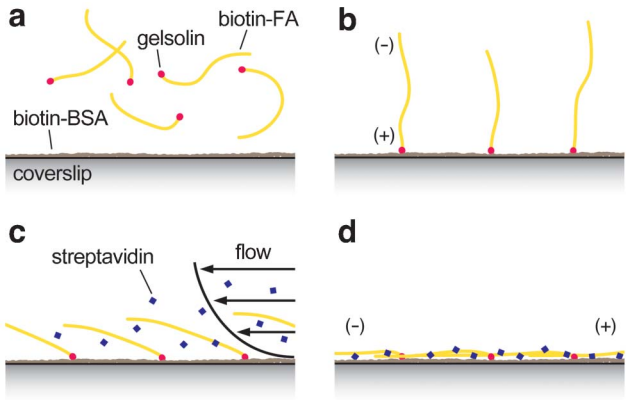

Fig. 1 Schematic procedure of assembling an isopolar array of actin filaments. (a) A solution containing filamentous actin (FA) terminated with gelsolin at the ''+'' end was infused into a flowchamber. The surface of the flowchamber had been coated with biotinylated BSA, and actin filaments had been sparsely decorated with biotin. (b) Actin filaments were anchored to the surface by gelsolin. Unbound filaments were washed out. (c) A shear flow containing streptavidin was imposed. The filaments were stretched and laid downstream of the buffer flow. (d) The filaments were immobilized on the surface *via* avidin-biotin conjugations.

Spudich *et al.*[27] utilized another capping protein, severin, to anchor the filaments *via* one end of the filament on a surface. Then, they applied buffer flow to trail the filaments parallel to the image plane and studied actin-myosin interactions under continuous flow. Recently, Yuan *et al.*[28] used poly-L-lysine, a polymer which has a counter (plus) charge against actin filaments, to immobilize oriented actin filaments on a glass surface *via* electrostatic interaction. However, the motor activity was diminished because of the effect of poly-L-lysine. The durability and stability of this actin array based on the electrostatic interaction were unknown as well. In our study here, we utilized gelsolin to anchor the filaments on a glass substrate *via* the plus ends, buffer flow to orient the filaments in parallel, and stable biotin-avidin conjugations to immobilize the filaments on the substrate (Fig. 1). From ATP-dependent unidirectional motion of myosin V, we confirmed that almost all (>99%) the filaments were oriented in the expected direction, and the immobilized filaments retained intact speed of myosin. Advantages of the actin-myosin system compared to the microtubule-kinesin system are discussed as well.

Results and discussion

Preparation of the gelsolin-actin complex

We first prepared the gelsolin-actin complex. For gelsolin, we prepared a Ca^{2+} insensitive mutant,[29,30] which caps the plus end of actin filament even in the absence of Ca^{2+}. This mutant enables one to use a variety of solution conditions. While gelsolin severs actin filaments and caps their plus ends, it is known that, in the presence of actin monomers, gelsolin recruits two actin monomers and nucleates actin assembly.[31] We utilized this property; we first mixed gelsolin with actin monomers in solution and increased the salt concentration to promote actin polymerization. A small amount of biotinylated actin monomer was also added to this mixture to prepare sparsely biotinylated actin filaments. We stabilized the polymerized actin filament by adding fluorescence-labeled phalloidin. We confirmed this complex is stable on ice for more than one month.

Parallel alignment of actin filaments

A flowchamber was assembled by placing two $\sim$50 μm thick spacers onto a KOH-washed coverslip (32 × 24 mm^2) with another coverslip (18 × 18 mm^2) on top. The gap between the two spacers was $\sim$5 mm and the inner volume of the chamber was $\sim$15 μL. To exchange the solution (or make flow described below), paper filters cut into a wedge shape were used. In the following procedures, the solution was infused into one side of the chamber and excess volume was drawn off by the paper filter from the outlet. First, the biotinylated-BSA solution was infused to coat the inner surface. Next, the gelsolin-capped actin filaments that had been sparsely biotinylated and fluorescently-labeled were injected (Fig. 1a). After a 3 min incubation, we found that the gelsolin-capped filaments bound to the surface at one end (Fig. 2a and the beginning of Movie S1, ESI†). We confirmed that the filaments were anchored to the surface through gelsolin (see below). Then, we imposed buffer flow containing streptavidin, which binds to four biotin molecules tightly ($K_d \sim 10^{-14}$ M)[32] (Fig. 2c and Movie S1, ESI†). The shear flow made the filaments stretch and lie down on the surface (Fig. 1c). Subsequently, the filaments got crosslinked to the surface *via* biotin-avidin conjugations (Fig. 1d). The flow rate was $\sim$15 μL s^{-1}, which was estimated by the total inlet volume divided by the exchange time. Finally, unbound streptavidin was washed out. Thus, we succeeded in orienting anchored filaments in parallel and immobilizing them on the glass surface. The length of the immobilized filament was 5.4 ± 3.8 μm (mean ± s.d., n = 134). The angle distribution (the angle of the vector connecting both ends of the immobilized filament) fits well with a Gaussian function and the standard deviation was 10.8° (n = 134). We confirmed that the gelsolin-capped actin filaments were attached to the surface through gelsolin as follows. We prepared actin filaments in the absence of gelsolin, and performed the same procedure as the actin orientation process. As mentioned, the gelsolin-capped actin filaments were bound to the surface at one end (Fig. 2a), while absorption of the uncapped filaments on the surface was not observed for almost all the parts of the surface (Fig. 2b). By comparing the density of gelsolin-capped and uncapped actin filaments attached on the surface (see Fig. 2a and 2b captions), we estimated that the probability of nonspecific absorption was $\sim$0.1%. Although the specificity of the connection between gelsolin and the surface is unclear, the connection was tight. In the flow rate ($\sim$15 μL s^{-1}) and time period ($\sim$5 s), less than 0.1% of actin filaments were detached from the surface. Moreover, we have never found the filaments detaching from the substrate on the usual observation time scale ($\sim$15 min) in the absence of flow.

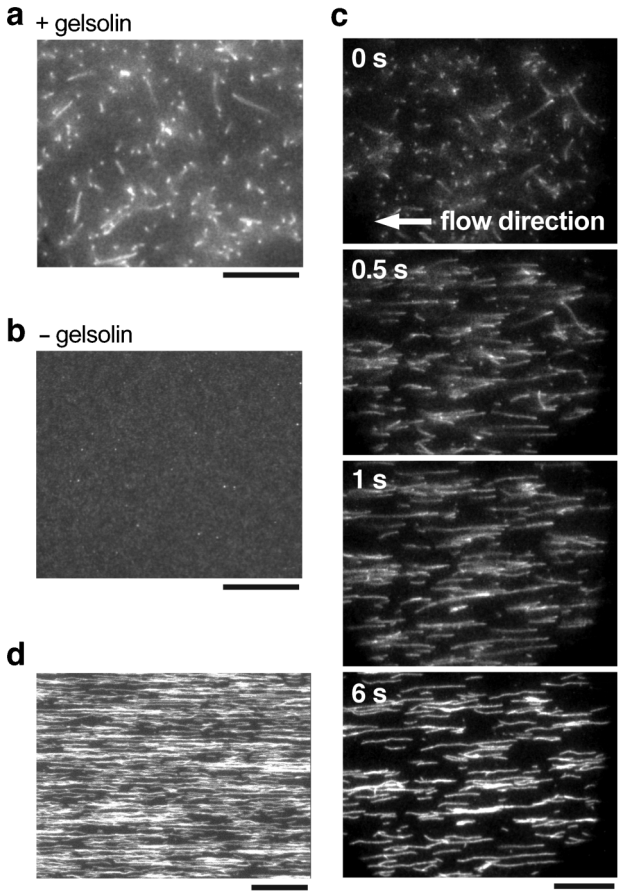

Fig. 2 Snapshots of the assembly process and the immobilization of actin filaments. All images focused on the bottom coverslip. (a, b) 0.2 μM of actin filaments capped with gelsolin (a) or uncapped (b) was incubated in a flowchamber for 3 min and the image was taken after unattached filaments were washed out by exchanging the solution. (a) The density of anchored filaments was 0.16 μm^{-2} [4.5 ± 3.4 (mean ± s.d.) filaments per 5 × 5 μm^2 (n = 60)]. (b) Less than 0.2 filaments were absorbed on the surface per field of view (~ 1570 μm^2), *i.e.*, the density of absorbed filaments was less than 1.27 × 10^{-4} μm^{-2}. (c) Sequential images of the actin filaments orientated by flow and surface immobilization by streptavidin. 0 s corresponds to the beginning of flow observed in the field of view (see also Movie S1, ESI†). 0.2 μM of actin solution with gelsolin was used. The line density of immobilized filaments perpendicular to the orientation of the flow was 0.62 μm^{-1} [6.2 ± 1.4 (mean ± s.d.) filaments per 10 μm (n = 34)]. (d) A dense array of actin filaments immobilized by biotin-avidin conjugation. 1 μM of actin solution was used. The line density of immobilized filaments perpendicular to the orientation of the flow was estimated to be 2.9 μm^{-1} based on the relation between the area density and the line density in the case of 0.2 μM actin and the assumption that the line density was proportional to the area density. Scale bars represent 10 μm.

For applications of this method, the time required to construct the system is important. The previously proposed method to assemble similar arrays of microtubules requires expertise in microfluidics to maintain constant flow over several minutes.[9,10] In their system, the fabrication process includes three biochemical/chemical reactions and take several tens of minutes for the assembly. In contrast, our method does not require precise control of buffer flow and takes less than ten minutes in total. This may be important for further applications, and may improve and stabilize the quality of products.

Density control of actin filaments

It is important to control the density of oriented actin filaments, especially for long distance transport. The reason is as follows. Single molecule studies on motor proteins have clarified that the run length of motor proteins (the moving distance of a single motor protein along the filament without detachment after the molecule encounters the filament) is a few micrometers at the longest. Therefore, to carry a cargo for a longer distance, multiple motor proteins attached to the same cargo have to interact with the oriented filaments simultaneously.[12,33] In this situation, a dense array which allows multiple motors to interact simultaneously with more than one filament may support longer transport. This principle seems to be realized in living cells, where so-called actin cables (bundles of multiple actin filaments) appear to be involved in transport processes.[33,34]

Our method allows one to construct the desired density of actin arrays easily by controlling the concentration of actin in solution. To show the capability to control the density, we first prepared different concentrations of gelsolin-capped actin filaments (0.1–5 μM actin, the molar ratio between actin and gelsolin was fixed) and then performed the same procedure as the surface anchoring process (Fig. 1a and 1b). We confirmed that the density of surface-anchored filaments was almost proportional to the concentration of the gelsolin-capped actin filament solution perfused into the flowchamber (Fig. 3). Subsequently, we performed the same procedure as the surface orientation process as described above. The parallel

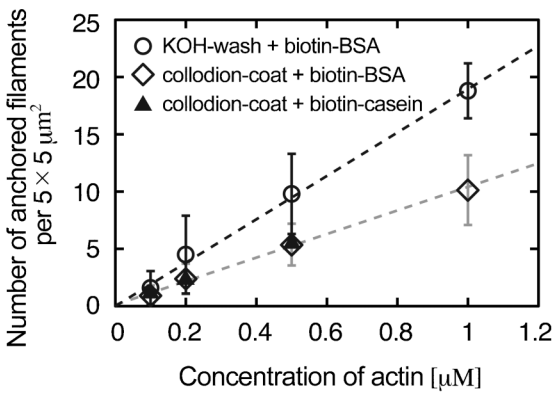

Fig. 3 Relationship between the concentrations of gelsolin-capped actin filaments imposed into the flowchamber and the area density of actin filaments attached to the glass surface. The molar ratio between actin and gelsolin was fixed, and the concentration of actin was varied. KOH-washed glass with a biotinylated BSA coat (circle), collodion-coated glass with a biotinylated BSA coat (diamond), and collodion-coated glass with a biotinylated casein coat (triangle) were each evaluated. Error bars indicate standard deviations and the dotted lines indicate linear fittings (black: KOH-washed glass with a biotinylated BSA coat, gray: collodion-coated glass with a biotinylated BSA coat). To evaluate the area densities of actin filaments, we counted up the number of anchored filaments in every 5 μm square field of view and took the average. For all data points, $n \geqslant 37$. For more than 1 μM actin, it was difficult to distinguish the anchored points of each filament one by one due to the high density.

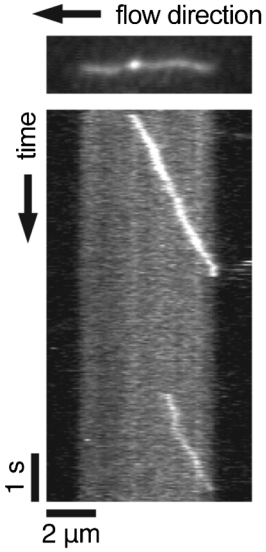

Fig. 4 Unidirectional motion of myosin V-coated fluorescent beads along the oriented actin filament. The top figure shows a snapshot image of an immobilized actin filament and a myosin V-coated bead (bright spot). 0.1 μM of actin filaments capped with gelsolin was used, and the orientation of flow had been imposed from right to left in this figure. If the actin filament was oriented correctly, the immobilized filament directed its plus end to the right (Fig. 1). In this case, because myosin V is a plus-end directed motor, the beads are supposed to move from left to right. The bottom kymograph shows the motion of myosin V-coated beads along the oriented actin filament. The beads moved from left to right, showing this actin filament was oriented in the correct direction. The first bead, shown also in the top figure, was detached at the end of the filament. The second bead bound to the filament after a few seconds.

arrays of actin filaments at the different densities from 0.06 μm^{-2} (Fig. 4) to 3.75 μm^{-2} (Fig. 2d) were successfully constructed. At high densities, non-specific absorption of the filaments before the surface immobilization process may often occur. Although that absorption took place, we observed that flexible actin filaments crossed over such obstacles easily. This result suggests that the actin filament is more suitable than the rigid microtubule for the fabrication of high-density array, which may be useful for long distance transport powered by motor proteins.

Actin polarities and cargo-transport activities

We confirmed polarities and cargo-transport activities of each filament immobilized on a substrate by ATP-dependent movement of myosin V that moves unidirectionally along the actin filament towards the plus end.[35,36] Myosin V molecules were attached to small fluorescent beads (ϕ = 0.01 μm), and the myosin V-coated beads were perfused into a flowchamber. Then, the chamber was sealed with silicon grease to prevent buffer flow. We utilized a thin array of actin filaments in order that individual actin filaments can be distinguished one by one. The beads moved along the filaments in one direction (Fig. 4). Since myosin V is a plus-end directed motor, the beads were expected to translocate in the upstream direction of the flow if the actin filaments were oriented in the correct direction. Indeed almost all of the beads translocated in the upstream direction. We counted the numbers of filaments that were oriented in the correct and incorrect directions over three different chambers and confirmed that the orientation accuracy was 99.6% (n = 264) (Table 1). In addition, we confirmed that the streptavidin molecules, which were sparsely bound to the immobilized actin filaments (see Fig. 1d), did not slow down the speed of myosin V. The velocity of myosin V-coated beads moving along the immobilized filaments was 0.62 ± 0.10 μm s^{-1} (mean ± s.d., n = 29), which was almost the same value without streptavidin.[37,38]

Table 1 Accuracy of the polarity alignment of actin filaments

Chamber no.	Correct	Incorrect	Accuracy (%)
1	118	1	99.1
2	106	0	100
3	39	0	100
Total	**263**	**1**	**99.6**

Since myosin V has two ''feet'' and translocates along an actin filament in a ''hand-over-hand'' fashion apparently like human walking,[39] it can easily step over small obstacles such as streptavidin molecules on the actin filament.[36]

Alternative methods for the surface immobilization of actin filaments and for the surface treatment of flow chambers

Providing alternative methods is important for the practical utility of this technique because optimal surface treatment of the flow channel and the cross-linker of actin filaments on the surface depend on the target molecules and the other parts of the chip.

For the immobilizing process of actin filaments on the surface, streptavidin could be replaced by α-actinin in the case of dense actin arrays. α-Actinin is an actin-binding protein that forms a dimer and crosslinks two actin filaments.[14] We prepared non-biotinylated actin filaments capped with gelsolin, and anchored the filaments through gelsolin to the glass surface pre-coated with biotinylated BSA. Then, buffer flow containing α-actinin was imposed into the chamber. As a result, actin filaments were successfully immobilized in the downstream direction (Fig. 5a). The line density of this array perpendicular to the orientation of the flow was estimated to be 14.5 μm^{-1} (see Fig. 5a caption). We note that the interaction between α-actinin and the surface is unclear. However, the dense isopolar array might be assembled by the filament crosslinking alone in the presence of flow; when the density of actin filaments is high enough so that the trailing end can crosslink with other filaments trailing in the downstream direction, the filaments (except for those at the end point of arrays) should be immobilized on the surface.

For surface treatment, a KOH-washed cover slip coated with biotinylated-BSA can be replaced by a collodion-coated cover slip coated with biotinylated-BSA, or a collodion-coated cover slip coated with biotinylated-casein. In both cases, actin filaments were anchored to the surface *via* gelsolin; the densities were proportional to the concentration of gelsolin-capped actin filaments in the solution perfused into the flowchamber (Fig. 3), while the absorption of uncapped actin filaments to the surface was blocked almost equally compared

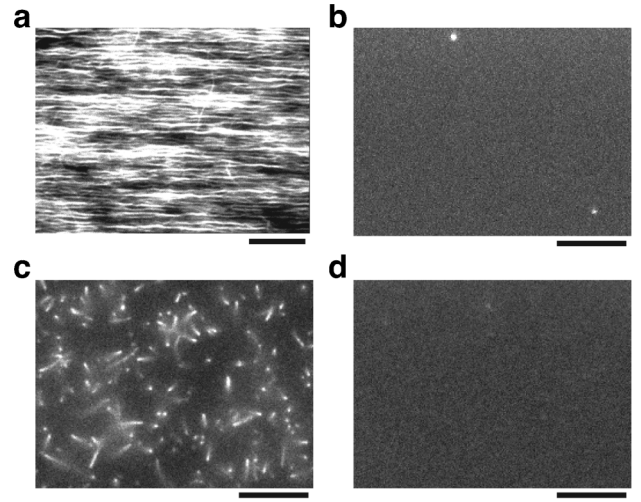

Fig. 5 Alternative methods of actin immobilization and surface treatment. (a) A dense array of actin filaments immobilized by α-actinin. 5 μM of the gelsolin-capped but not biotinylated filaments was used. The line density of immobilized filaments perpendicular to the orientation flow was 14.5 μm^{-1}, which was estimated by the same method as in Fig. 2d. (b) Surface binding of the gelsolin-capped actin filament was blocked by replacing the surface coating with non-biotinylated BSA, compared with Fig. 2a. A KOH-washed glass and 0.2 μM of the gelsolin-capped actin was used. (c, d) Surface binding of the gelsolin was controlled by (c) the presence or (d) the absence of an anti-His antibody. After the immobilization of the antibody, the surface was coated with casein. A collodion-coated glass and 1 μM of the gelsolin-capped actin was used. Scale bars represent 10 μm.

to the case of a KOH-washed cover slip coated with biotinylated-BSA (Fig. 2b). In all cases, actin filaments were successfully aligned on the surface by buffer flow with streptavidin. Moreover, the histidine-tag on our gelsolin mutant could be utilized to specifically fix the molecule on the surface. Indeed, binding of gelsolin-capped actin filaments to the surface was controlled by an anti-His antibody (Fig. 5c and 5d). A different tag or anti-gelsolin antibody may also be utilized.

Collectively, we demonstrated two ways of the surface immobilization of the actin filament and four ways of the surface treatment of flow channels. Such variations allow one to choose the best method for one's application.

In addition, surface binding of gelsolin-capped actin filaments, namely both gelsolin and actin filaments, was blocked by the coating of (non-biotinylated) BSA on a KOH-washed glass (Fig. 5b) or by the coating of (non-biotinylated) casein on a collodion-coated glass (Fig. 5d). Therefore, based on these methods, a patterned array of actin filaments can be fabricated;[25] using a microprinting technique of coating only a part of a chip surface by biotinylated-BSA or biotinylated-casein and the rest by normal BSA or casein enables one to anchor gelsolin-capped actin filaments to desired locations.

Advantages of the actin-myosin system

Compared to the microtubule-kinesin system, the actin-myosin system may have several advantages for motor-protein driven transport systems. First, the actin filament allows faster transport because myosin XI is known as the fastest molecular motor (60–100 μm s^{-1}) among all actins or microtubule associated motor proteins that have been previously characterized (as far as we know).[40,41] Second, the actin filament allows one to downsize a fluidic device. As mentioned, the actin filament is 100 times more flexible than the microtubule. Therefore, precise wiring in a serpentine nano-channel with a small curvature is easier, which helps the sophisticated integration of a flow circuit onto a smaller chip. Finally, as discussed above, the actin filament is more suitable than the rigid microtubule for long distance transport because high flexibility of the actin filament may be suited for the assembly of dense arrays of tracks of motor proteins. Indeed, dense actin arrays up to 2.9 μm^{-1} (immobilized by streptavidin; Fig. 2d) and 14.5 μm^{-1} (immobilized by α-actinin; Fig. 5a) were successfully fabricated. Thus, at least, submicron-sized cargos can be transported by multiple motor proteins along different filaments simultaneously.

Conclusion

In this study, we established a method to assemble an isopolar array of actin filaments applicable to motor-protein driven transport systems. The polarities of aligned filaments and cargo-transport capability were evaluated by the unidirectional movement of myosin molecules. Indeed, 99.6% of the filaments were oriented in the correct direction, and the array retained the speed of myosin previously reported.[37,38] Our method is quick: the fabrication process requires less than ten minutes. Moreover, this method allows one to optimize the transport capability by controlling the actin density. Finally, multiple alternative methods were provided for the fabrication process which is essential for diverse applications requiring different conditions; two alternative ways of the surface immobilization of the actin filament, four alternative ways of the surface treatment of flow channels, and two ways of the surface treatment to block binding of gelsolin-actin complex were demonstrated.

Our study is a fundamental step toward the development of myosin driven transport systems inside flow channels. Since our actin array may have great advantages for downsizing of a fluidic device to the nanoscale, we hope our actin array contributes to further development of a nano total analysis system.

Acknowledgements

The authors thank A. Weeds for the original gelsolin clone, Y. Y. Toyoshima for the gelsolin mutant, Y. Oguchi and H. Kubota for help with myosin V purification, Y. Shimamoto for help with actin purification, M. Shio for designing a stable microscope stage, and K. Adachi for an image analysis program. The authors also thank the members of Kinosita lab for helpful advice and M. Fukatsu and K. Sakamaki for lab management and encouragement, and T. Z. Jia for careful reading of the manuscript. This work was supported in part by

Grant-in-Aid for Young Scientists(B) (M.M.) and Grant-in-Aid for Scientific Research(C) (K.S.) from the Japanese Society for the Promotion of Science, and Specially Promoted Research from the Ministry of Education, Culture, Sports, Science, and Technology of Japan.

References

1 D. R. Reyes, D. Iossifidis, P.-A. Auroux and A. Manz, *Anal. Chem.*, 2002, **74**, 2623–2636.
2 P.-A. Auroux, D. Iossifidis, D. R. Reyes and A. Manz, *Anal. Chem.*, 2002, **74**, 2637–2652.
3 P. S. Dittrich, K. Tachikawa and A. Manz, *Anal. Chem.*, 2006, **78**, 3887–3908.
4 J. West, M. Becker, S. Tombrink and A. Manz, *Anal. Chem.*, 2008, **80**, 4403–4419.
5 M. U. Kopp, A. J. de Mello and A. Manz, *Science*, 1998, **280**, 1046–1048.
6 C. Yi, C.-W. Li, S. Ji and M. Yang, *Anal. Chim. Acta*, 2006, **560**, 1–23.
7 S. B. Cheng, C. D. Skinner, J. Taylor, S. Attiya, W. E. Lee, G. Picelli and D. J. Harrison, *Anal. Chem.*, 2001, **73**, 1472–1479.
8 P. S. Dittrich and A. Manz, *Nat. Rev. Drug Discovery*, 2006, **5**, 210–218.
9 R. Yokokawa, S. Takeuchi, T. Kon, M. Nishiura, K. Sutoh and H. Fujita, *Nano Lett.*, 2004, **4**, 2265–2270.
10 R. Yokokawa, Y. Yoshida, S. Takeuchi, T. Kon and H. Fujita, *Nanotechnology*, 2006, **17**, 289–294.
11 V. Mermall, P. L. Post and M. S. Mooseker, *Science*, 1998, **279**, 527–533.
12 T. Shimmen, *J. Plant Res.*, 2007, **120**, 31–43.
13 N. Hirokawa, *Science*, 1998, **279**, 519–526.
14 *Molecular Biology of the Cell*, ed. B. Alberts, A. Johnson, J. Lewis, M. Raff, K. Roberts and P. Walter, Garland Science, New York, 5th edn, 2007, Ch. 16.
15 *Mechanics of Motor Proteins and the Cytoskeleton*, ed. J. Howard, Sinauer Associates Inc, Sunderland, Massachusetts, 2001, Ch. 7.
16 T. Yanagida, M. Nakase, K. Nishiyama and F. Oosawa, *Nature*, 1984, **307**, 58–60.
17 A. Ott, M. Magnasco, A. Simon and A. Libchaber, *Phys. Rev. E: Stat. Phys., Plasmas, Fluids, Relat. Interdiscip. Top.*, 1993, **48**, R1642–R1645.
18 R. Yasuda, H. Miyata and K. Kinosita Jr, *J. Mol. Biol.*, 1996, **263**, 227–236.
19 Y. Arai, R. Yasuda, K. Akashi, Y. Harada, H. Miyata, K. Kinosita Jr and H. Itoh, *Nature*, 1999, **399**, 446–448.
20 B. Mickey and J. Howard, *J. Cell Biol.*, 1995, **130**, 909–917.
21 R. Stracke, K. J. Böhm, J. Burgold, H.-J. Schacht and E. Unger, *Nanotechnology*, 2000, **11**, 52–56.
22 K. J. Böhm, R. Stracke, P. Mühlig and E. Unger, *Nanotechnology*, 2001, **12**, 238–244.
23 I. Prots, R. Stracke, E. Unger and K. J. Böhm, *Cell Biol. Int.*, 2003, **27**, 251–253.
24 L. Limberis, J. J. Magda and R. J. Stewart, *Nano Lett.*, 2001, **1**, 277–280.
25 L. Huang, P. Manandhar, K.-E. Byun, P. B. Chase and S. Hong, *Langmuir*, 2006, **22**, 8635–8638.
26 N. Suzuki, H. Miyata, S. Ishiwata and K. Kinosita Jr, *Biophys. J.*, 1996, **70**, 401–408.
27 J. A. Spudich, S. J. Kron and M. P. Sheetz, *Nature*, 1985, **315**, 584–586.
28 J. Yuan, A. Pillarisetti, Y. E. Goldman and H. H. Bau, *Nano Lett.*, 2013, **13**, 79–84.
29 K.-M. Lin, M. Mejillano and H. L. Yin, *J. Biol. Chem.*, 2000, **275**, 27746–27752.
30 K. Shiroguchi, M. Ohsugi, M. Edamatsu, T. Yamamoto and Y. Y. Toyoshima, *J. Biol. Chem.*, 2003, **278**, 22460–22465.
31 P. A. Janmey, C. Chaponnier, S. E. Lind, K. S. Zaner, T. P. Stossel and H. L. Yin, *Biochemistry*, 1985, **24**, 3714–3723.
32 N. M. Green, *Adv. Protein Chem.*, 1975, **29**, 85–133.
33 M. P. Sheetz and J. A. Spudich, *Nature*, 1983, **303**, 31–35.
34 N. Kamiya, *Annu. Rev. Plant Physiol.*, 1981, **32**, 205–236.
35 *Mechanics of Motor Proteins and the Cytoskeleton*, ed. J. Howard, Sinauer Associates Inc, Sunderland, Massachusetts, 2001, Ch. 13.
36 K. Shiroguchi and K. Kinosita Jr, *Science*, 2007, **316**, 1208–1212.
37 J. N. Forkey, M. E. Quinlan, M. A. Shaw, J. E. T. Corrie and Y. E. Goldman, *Nature*, 2003, **422**, 399–404.
38 S. Uemura, H. Higuchi, A. O. Olivares, E. M. De La Cruz and S. Ishiwata, *Nat. Struct. Mol. Biol.*, 2004, **11**, 877–883.
39 A. Yildiz, J. N. Forkey, S. A. McKinney, T. Ha, Y. E. Goldman and P. R. Selvin, *Science*, 2003, **300**, 2061–2065.
40 S. Higashi-Fujime, R. Ishikawa, H. Iwasawa, O. Kagami, E. Kurimoto, K. Kohama and T. Hozumi, *FEBS Lett.*, 1995, **375**, 151–154.
41 M. N. Rivolta, R. Urrutia and B. Kachar, *Biochim. Biophys. Acta, Bioenerg.*, 1995, **1232**, 1–4.